JEE Journal of Ecological Engineering

Journal of Ecological Engineering 2023, 24(10), 259–276
https://doi.org/10.12911/22998993/169176
ISSN 2299–8993, License CC-BY 4.0

Received: 2023.06.13
Accepted: 2023.07.03
Published: 2023.08.24

Date Palm Fibre Waste Exploitation for the Adsorption of Congo Red Dye via Batch and Continuous Modes

Qahtan Adnan Ali[1], Mohammed Ali A. Shaban[2], Sabah J. Mohammed[3], Mohanad J. M-Ridha[4], Hussein H. Abd-Almohi[5], Khalid M. Abed[6,7], Muhammad Zulhaziman Mat Salleh[8], Hassimi Abu Hasan[8,9*]

[1] Department of Environment and Pollution Techniques Engineering, Technical Engineering College, Kirkuk, Northern Technical University, 36001 Kirkuk, Iraq
[2] Civil Engineering Department, College of Engineering, Al-Nahrain University, Baghdad, Iraq
[3] Department of Environmental, North Refineries Company (NRC), Ministry of Oil, Baiji, Salahuldeen, Iraq
[4] Department of Environmental Engineering, College of Engineering, University of Baghdad, Baghdad, Iraq
[5] Department of Oil Engineering, Al-Farabi University College, Baghdad, Iraq
[6] Department of Chemical Engineering, College of Engineering, University of Baghdad, Baghdad, Iraq
[7] Department of Chemical Engineering, Faculty of Engineering, Universiti Malaya, Kuala Lumpur 50603, Malaysia
[8] Department of Chemical and Process Engineering, Faculty of Engineering and Built Environment, Universiti Kebangsaan Malaysia, 43600 UKM Bangi, Selangor, Malaysia
[9] Research Centre for Sustainable Process Technology (CESPRO), Faculty of Engineering and Built Environment, Universiti Kebangsaan Malaysia, 43600 UKM Bangi, Selangor, Malaysia
* Corresponding author's e-mail: hassimi@ukm.edu.my

ABSTRACT

The present study utilised date palm fibre (DPF) waste residues to adsorb Congo red (CR) dye from aqueous solutions. The features of the adsorbent, such as its surface shape, pore size, and chemical properties, were assessed with X-ray diffraction (XRD), BET, Fourier-transform infrared (FTIR), X-ray fluorescence (XRF), and field emission scanning electron microscope (FESEM). The current study employed the batch system to investigate the ideal pH to adsorb the CR dye and found that acidic pH decolourised the dye best. Extending the dye-DPF waste mixing period at 25 °C reportedly removed more dye. Consequently, the influence of the starting dye and DPF waste quantity on dye removal was explored in this study. At 5 g/L dye concentration, 48% dye removal was achieved, whereas at low dye concentrations, only 40% of the dye was removed. The current study also evaluated the DPF particle size created for dye adsorption, yielding a 66% optimal powder size removal. The heat impact assessment performed in this study indicated that increased temperature affected the amount of dye eliminated from aqueous solutions, where a 72% removal was recorded at 45 °C. The pseudo-first- and pseudo-second-order models were utilised to predict the maximum CR dye adsorption with DPF waste. Resultantly, the Langmuir-Freundlich experimental DPF waste CR adsorption documented pseudo-second-order kinetics. In a fixed bed reactor, the DPF waste has been reported to remove CR dye constantly. Consequently, several factors affecting the removal process, including the effects of primary dye, the flow rate of the liquid inside the column, the depth of the filling inside the column, and flow rate were assessed. The results were simulated in the COMSOL® program and compared to practical experiments, which yielded a 99% match. Conclusively, DPF waste could remove several colours from wastewater via active removal.

Keywords: adsorption, Congo red dye, batch adsorption, continuous adsorption, COMSOL.

INTRODUCTION

In recent years, water pollution due to leakages of significant amounts of poisonous dyes, heavy metals, chemical, and biological contaminants from different sectors into the groundwater and surface water, has become a serious environmental issue (Hasan and Ahamd, 2019). Although the textile sector primarily utilises the majority of dyes manufactured globally, dyes are also widely employed in numerous manufacturing industries, including fabrics, skincare, wood, plastic materials, printers, insecticides, petrochemical, paintings, and medicines (Chebli et al., 2014).

Dyes are among the major contaminants in wastewater that are significantly harmful to humans as they are permanent and non-biodegradable. Consequently, the polluted water from the industrial sectors, which includes dyes discharged into the water flow, also impacts the ecosystem (Subramaniam and Kumar Ponnusamy, 2015). The hazardous chemical by-products in the dyes do not only have adverse effects on human health and the environment, but the colours in the dyes might disrupt photosynthetic activities, where they obstruct sunlight paths through water layers, preventing the light from reaching aquatic creatures and plants (Chan et al., 2016; Yagub et al., 2012). Consequently, the dye-polluted water requires treatment to remove the environmentally damaging substances.

Researchers have been seeking alternative, environmentally friendly, and low-cost approaches to remove dyes from water. Several methods for removing colours from wastewater include coagulation/flocculation (Zhou et al., 2014), oxidation/ozonation (Malik and Saha, 2003), membrane separation (Ciardelli et al., 2001; Tan et al., 2015), photodegradation (Gardiner and Borne, 1978), and biological process (Ledakowicz et al., 2001). Nevertheless, most of the traditional approaches are ineffective and typically costly (Chen et al., 2013). Adsorption technology is one of the most common, desirable, and available technologies for removing dyes. Nonetheless, although activated carbon has been acknowledged as one of the finest techniques to treat the water contaminated by biological and chemical contaminants due to its wide contact area and a large adsorption capacity, the method is very expensive (Ahmad and Alrozi, 2011; Depci et al., 2012).

Typically, the wastewater from painting paper mills and pharmaceutical plants contains cationic dyes (Zhang et al., 2013). Congo Red (CR) ($C_{32}H_{22}N_6Na_2O_6S_2$) is the most widely employed dye in the industry. However, CR in wastewater is an issue, since it harms the environment and human health. Consumption of the water containing CR dye could cause symptoms such as vomiting, tissue necrosis, and cyanosis in humans. Consequently, the World Health Organization (WHO) recommended removing the dye from wastewater (Al-bayati and Najim, 2022).

Well water or groundwater is the primary source of water for a majority of the global population, particularly in dry regions. In Iraq, approximately 50% of fresh water is obtained from clean groundwater. The source also supplies around 56% of the water consumed in the United States. Groundwater refers to the water gathered under soil. The water is deposited from outside surfaces due to geological formations on earth. Nonetheless, the water is often contaminated with CR dye from industries and other human activities. Groundwater pollution significantly impacts the nations that rely on the water source as their clean water source.

Low permeability barrier (LPB) and extraction wells could be employed for waste containment in underground environments to limit the on-site movements of water and restrict off-site activities of different molecules. Large amounts of liquid could infiltrate landfills via irrigated agriculture or precipitation, thus, the water movements in the waste material layers would produce effluents accumulating upon the liners. Nevertheless, liner failures due to any reason would result in leachates entering the natural areas, contaminating soil and groundwater. Consequently, containment vessels are necessary to preserve the subterranean regimes. The system must include a bottom liner and a landfill cover to avoid water intrusion.

Numerous researchers have examined alternative ionic dyes adsorption approaches. For example, Zhang et al. (2013) (Zhang et al., 2013) examined the viability of removing cationic dyes from wastewater by adsorbing them onto sugar cane, while Yagub et al. (2012) (Yagub et al., 2012) adsorbed colours from water onto pine trees. Another study (Chan et al., 2016) employed other species, including pineapple as adsorbents. Consequently, the technique eschewed the utilisation of activated carbon in favour of safer and cheaper methods. Adsorption is also advantageous when employed to purify raw wastewater, as it reportedly reduces operating cost, eliminates

complicated organic compounds, and produces low residue levels (Saravanan et al., 2020).

Mesopotamia is distinguished by its palm trees, particularly in the southern parts. Palm plants comprise of trunks, peduncle bases, fronds, and thorns (fruits). During the harvest season, palm trees produce significant date waste that is often employed as animal feed, burnt or buried, which might be detrimental to the environment (Abed et al., 2022). Nevertheless, the wastes could be utilised for the adsorption of cationic dyes in water.

Considering that dyes are dangerous to human health, the current study aimed to purify the groundwater that has been directly or indirectly exposed to pollution. This study evaluated the potential of palm waste fibres to absorb the CR dye from contaminated ground water. The adsorption process was examined, and contemporary molecular-level interpretations were offered. The comprehensive examination of experimental and theoretical data revealed novel understanding of the adsorption of the dye with the materials procured. Moreover, the results yielded the outcomes describing the qualities of the adsorbent.

The current study performed CR dye removal via batch process at a laboratory level and determined the different conditions that could affect the removal efficiency from groundwater. Subsequently, a fixed-bed reactor adsorption system was evaluated empirically in a research facility tower under restricted operating conditions. A one-dimensional (1D) simulation was also created in COMSOL® Multiphysics to investigate the CR removal effectiveness and adsorption bed saturating duration. Subsequently, the model was verified in accordance with the experimental observations obtained.

MATERIALS AND METHODS

Adsorbate

A gram of the CR dye (CAS number 573-58-0, molecular weight: 696.66 g/mol, maximum absorbance: 498 nm; Sigma-Aldrich) was dissolved in a litre of distilled water in a volumetric flask to obtain a dye at a 1,000 ppm concentration. Alternatively, the appropriate amount of adsorption solution was first dissolved in distilled water, allowing the desired concentration to be attained. Subsequently, hydrochloric acid or sodium hydroxide (Sigma-Aldrich) was added to the dye solution to achieve the desired pH value.

Preparing and characterising the date palm fibre adsorbent

Discarded date palm fibre (DPF) wastes were gathered from Iraqi agricultural areas in the southern district of Baghdad. The materials were then rinsed with distilled water to completely eliminate any contaminants before being ambient air-dried for 24 h. Subsequently, the DPF were heated at 60 °C for 24 h. The waste material was then crushed and sieved with a 0.45 µm-pore membrane (Whatman, Germany) to remove the particles between 125 and 250 µm long. Next, the DPF waste fraction was washed numerous times with distilled water and dried at 48 °C for 48 h. When completely dried, the adsorbent was kept in airtight containers.

The present study employed an XRF spectrometer (ZSX Primus II) to determine the elemental structure of the DPF adsorbent obtained. On the other hand, the surface chemistry groups of the material were assessed with a Nicolet iS5 FT-IR spectrometer (Thermo Scientific) at a 550–4000 cm^{-1} scanning spectrum. Moreover, this study employed a surface area and porosity analyser (Micromeritics, ASAP 2020) with nitrogen adsorption at 77 K to calculate the surface areas of the adsorbents. The surface morphologies of the adsorbents were also observed through FESEM at a 12.5 kV accelerating voltage.

The batch experiments

During the thermal and an adsorption kinetic analyses of this study, the impacts of the major factors on the adsorption capabilities of the adsorbent, including pH, treatment time, starting dye concentration, and temperature, were determined. Mixtures of 100 mL of the CR dye and 0.3 g of every adsorbent prepared were filled in conical flasks before being shaken in a shaker (Grant Instruments Ltd) at 25 °C and 150 rpm. After a certain period, the samples were centrifuged. The concentration of dyes in the liquid phases was assessed with an ultraviolet-visible spectrophotometer (UV-Vis) (Shimadzu UV-1800, Japan) at 668 nm. The quantity of dye adsorbed at equilibrium was determined according to equations (Abed et al., 2022; Saravanan et al., 2020).

$$q_e = \frac{(C_o - C_e) * V}{m} \quad (1)$$

$$\text{RE}\% = \frac{C_o - C_e}{C_o} \quad (2)$$

where: C_o and C_e (mg/L) – the initial and the equilibrium liquid-phase dye concentrations, respectively;
V – the volume of the solution (L);
m – the mass of adsorbents (g).

The continuous experiments

This study assessed the possibility and ability of DPF waste to continuously remove dyes from wastewater. A fixed bed reactor containing the prepared DPF adsorbent was designed with plexiglass plates of a 6.157 × 10^{-6} m^2 cross-section area and 0.1 m deep, as shown in Figure 1. The specifications of the fixed bed reactor are listed in Table 1. In the system, the DPF waste was reinforced from the top and bottom with 10 cm of sand from Iraqi soil, which served as the porous media. The soil particles employed varied from 0.075 to 1.18 mm at an average diameter (d50) of 0.43 mm. The soil was primarily composed of silica (up to 94%) and clay elements, since bentonite is the main component in the World Food Summit.

Table 1. The properties of Iraqi soil used in this study

Property	Value Iraqi soil
Sand (%)	96.5
Hydraulic conductivity (cm/s)	$2.2 \cdot 10^{-3}$
Cation exchange capacity (meq/100 g)	2.13
pH	7.7
Bulk density (g/cm^3)	1.39
Organic content (%)	0.26
Porosity	0.47

The CR dye-contaminated solution prepared in this study was introduced from the bottom of the sand fill in the fixed bed reactor at different concentrations (10, 25, and 50 mg/l) and flow rates (25, 50, and 125 ml/min) to assess the aspects affecting the adsorption process. Water samples were then collected from different sectors of the reactor system every 5 min for 405 min. Subsequently, the dye concentrations of the samples were immediately determined with UV-vis.

During the continuous experiments in this study, the adsorbent particle size in the reactor was maintained at 0.0007 m. Sampling sites were installed at three areas denoted as ports 1, 2, and 3. The initial concentration of the contaminated solution before being introduced into the fixed-bed reactor was gathered at port 1, while port 2 allowed the collection of the CR-polluted solution after the liquid had flowed 50% of the

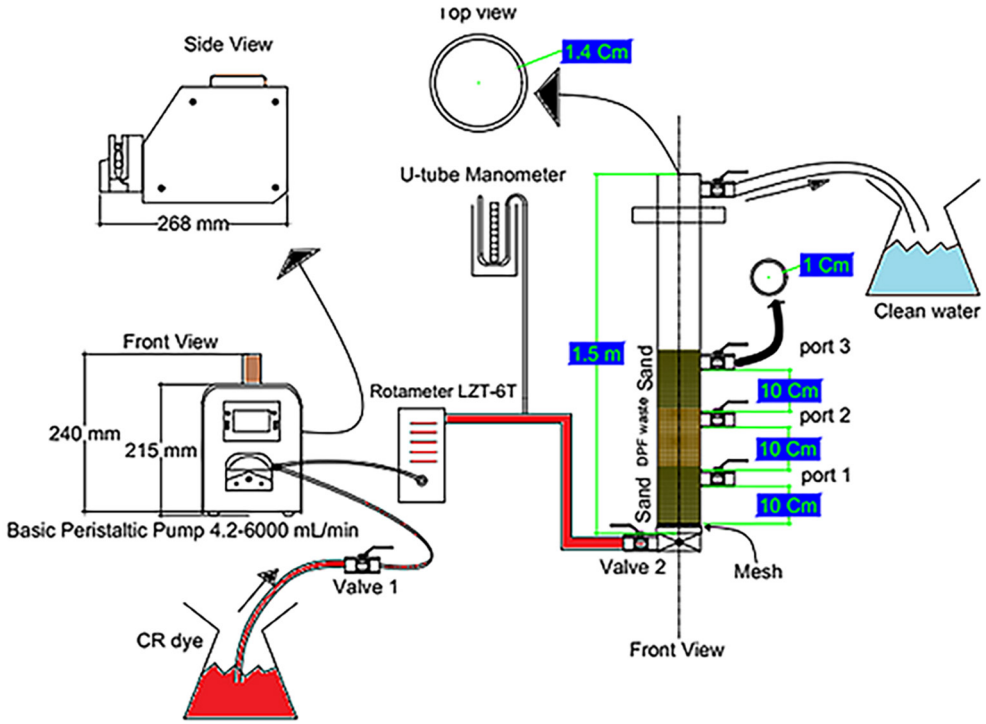

Figure 1. Schematic diagram for components of the experimental set-up

column height. At port 3, the concentration of the CR-contaminated solution post-flowing 100% of the column height was accumulated. The collection of the samples from the ports allowed monitoring of the CR adsorption process by the DPF waste adsorbent.

Initial CR-polluted solutions at 25 mg/L at 25, 75, and 125 L/min flow rates, a 50 mg/L solution at 25 L/min, and 50 mg/L at 25 L/min were introduced to the reactor with a peristaltic pump. The assessments in this study were conducted at room temperature. The CR-containing solution samples in this study were withdrawn at the sampling ports with stainless steel needles. The concentrations of removed pigments from the samples were determined by spectrophotometer analysing the dye interactions or influence on the dye solution or adsorbent in 2 mL amounts for each sample tested.

The current study designed a simulation model for a 10 cm-tall fixed-bed system with the COMSOL® program. The program employed physics-based built-in features to generate meshes suitable for the selected parameters. The quality and effectiveness of the design was evaluated through numerous indicators specified. For example, orthogonality is a critical quality standard. Cell deviations and vectors from the cell centre point to each face and their corresponding region vectors and the vector from the centroid of the cell to the centroids of each adjacent cell determine the criteria. For this study, the minimal diagonal quality for all cellular processes was set to over 0.01, with a substantially higher mean value. The numerical data for the critical mesh obtained in this study are summarised in Table 2.

While considering the mix occurring in the aqueous phase, the pressure gradient of the aqueous phase was assumed unchanged during the continuous mode operation conducted in the current study. Moreover, the temperature was presumed identical across each experiment. The CR adsorbed from the aqueous solutions was analysed with the COMSOL® simulation before employing the "saturated solute transport" modelling technique. The interaction offered a condensed modelling environment to analyse and assess different molecule developments, which were diffused across the ecosystem.

Table 2. Numerical data for the critical mesh

No.	Parameter	value
1	Sequence selected in COMSOL®	Physics-controlled mesh
2	Element size	fine
3	Shape of elements	Triangular
4	Edge elements	2431
5	Maximum growth rate	0.125 L/min
6	Average growth rate	0.075 L/min
7	Expressions	8

The expected diluted species were recorded at the physical interface, indicating that the quantities of the substances were significantly lower than those of a solid or liquid medium. The 1D equation for the COMSOL simulation is represented by Equation (3) (Solangi et al., 2022).

$$D_z \frac{\partial^2 C}{\partial Z^2} - V_z \frac{\partial C}{\partial Z} \mp \frac{r}{n} = \frac{\partial C}{\partial t} \tag{3}$$

$$r = -\rho_b \frac{\partial q}{\partial t} \tag{4}$$

The formula describes transport operations and conversion. Nonetheless, the final step is indicated by the response term r of the equation. The phrase is replaced by a plus sign, denoting the pollution sources, and a minus symbol, corresponding to the sink reactions. The removal of pollutants within the tower was governed by adsorption, reflected by the negative sign in Equation (4) (Nouh et al., 2010). From Equations (3) and (4):

$$D_z \frac{\partial^2 C}{\partial Z^2} - V_z \frac{\partial C}{\partial Z} = \frac{\partial C}{\partial Z} + \frac{\rho_b}{n} \frac{\partial q}{\partial t} \tag{5}$$

The general Langmuir formula could be represented as follows:

$$q_e = \frac{q_{max} b C_e}{1 + b C_e} \tag{6}$$

From equation 5 and 6 find that:

$$D_z \frac{\partial^2 C}{\partial Z^2} - V_z \frac{\partial C}{\partial z} = \left(1 + \frac{\rho_b}{n}\left(\frac{q_m\, b}{(1 + bC)^2}\right)\right)\frac{\partial C}{\partial t} \tag{7}$$

The formula was quantitatively determined with COMSOL® Multiphysics, which depended on the finite element technique, where n is the porosity of adsorption in the packed column and ρ_b denotes the bulk density of the bed (kg/cm^3).

RESULTS AND DISCUSSION

Adsorbent characterisation

The Fourier-transform infrared analysis

The Fourier-transform infrared (FTIR) is a straightforward and trustworthy method employed extensively in molecular and elemental chemicals as well as experimental and industrial processes. The technique is utilised extensively in quality assurance and fluid assessments. The FTIR results of both samples (before and after adsorption) in the current study were almost identical. The data obtained also demonstrated numerous adsorption regions, as indicated in Figure 2, which depicts the DPF waste sample before and after being employed in the adsorption process. The results demonstrated the differences between the surface characteristics of the organic compounds prior and after adsorption (Mohammed and Mohammed-Ridha, 2021).

The DPF waste sample in the present study recorded different FTIR apparent peaks, one of which was at 3797.2 cm^{-1}, attributable to the O-H group (3213.41–3863.42 cm^{-1}) (Uddin et al., 2017). The vibrational O-H bond peaks have been documented in substances including water, dyes, alcohols, and phenols. Another peak was observed at 2921 cm^{-1}, which corresponded to the carbohydrate (C-H) group (2920–2844 cm^{-1}) (Zhang et al., 2011). The findings might be due to the presence of aliphatic compounds-containing fatty groups. A peak documented with a 1733 cm^{-1} wavelength was consistent with the C=H bond Ca16 zha11, the group of carbohydrates between 1725–1745 cm^{-1}. New transitions were also observed at 1733, 2356, 1958, and 1945 cm^{-1}. The values indicated potential interactions between the DPF waste and the CR dye. Generally, spectral bands under 1000 cm^{-1} (Belala et al., 2011) indicate metal oxides.

The field emission scanning electron microscopy analysis

The field emission scanning electron microscopy (FESEM) is an electron microscopy method that produces high-resolution images of the surfaces of samples by directing a focused beam of electrons onto the samples. The technique could reveal the structural, shape, and compositional information of the materials assessed at minute scales. Furthermore, FESEM possesses a wide application range, including examinations of material microstructures, nanoparticle surface characterisations, and biological surface feature evaluations. Consequently, the approach is frequently employed in research and development in materials sciences, physics, as well as engineering field and in industrial settings to assess quality and detect failures (M-Ridha et al., 2022).

The surface structure of the DPF waste samples in the current study was observed through FESEM in a laboratory of the Ministry of Science and Technology in Baghdad, Iraq. Figure 3a illustrates the surface conditions of the DPF waste

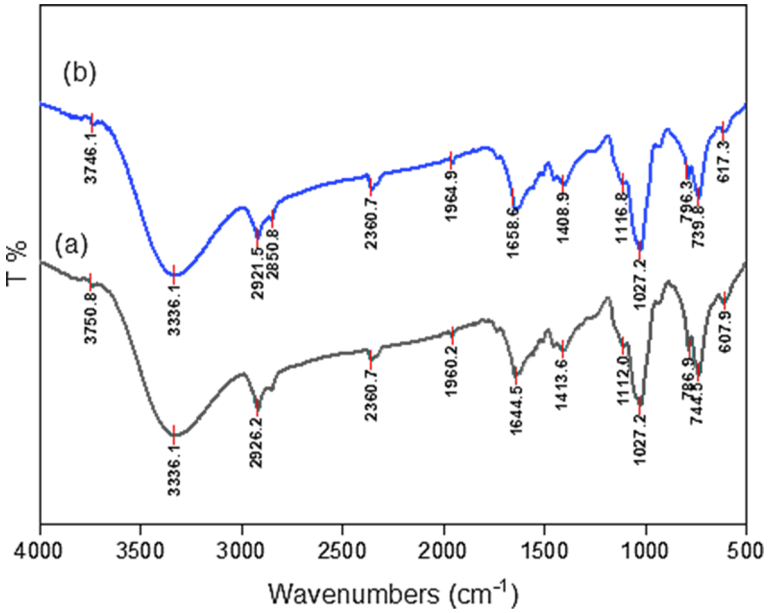

Figure 2. FTIR analysis (a) raw DPF and (b) CR adsorption by DPF

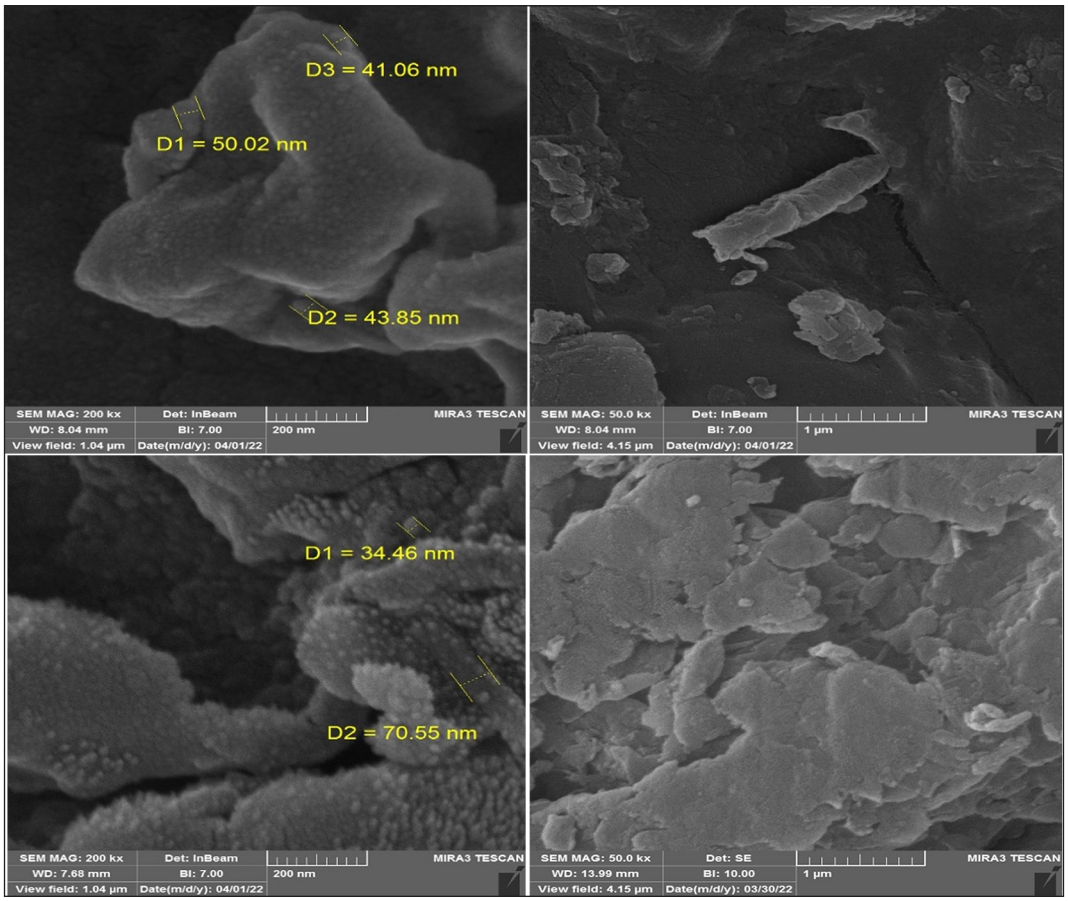

Figure 3. FESEM analysis (a) raw DPF and (b) CR adsorption by DPF

before it was employed to adsorb the CR dye, while Figure 3b depicts the sample after being utilised. The maximum pore of the DPF waste sample, before it was employed, was within the 41–50 nm range, but after adsorption, the pores were between 34 and 70 nm. Furthermore, the pores of the used DPF waste sample were filled with the CR dye. The results demonstrated that decreasing the surface area of the sample increased its contact area with the liquid, which ultimately enhanced the amount of dye adsorbed from the liquid.

The BET assessment

BET analysis measures the permeability of a structure by analysing the adsorption of a gas

Table 3. Specific BET characterization for DPF

Sample weight	0.0634	[g]
Cold free space	34.6184	[cm^3]
Worm free space	11.4473	[cm^3]
Equilibrium time	10	[sec]
Adsorption temperature	-196.15 °C	
Adsorptive	N2	
Surface area	0.7502	m^2/g
BET plot		
q·alpha/Qm	0.307	[cm^3(STP) g^{-1}]
Average particle size	5815.9661	Nm
BET area surface	0.1687	[m^2 g^{-1}]
Qm.C	0.0039	[cm^3(STP) g^{-1}]
Total pore volume (p/p_0=0.990)	0.016	[cm^3 g^{-1}]
Mean pore diameter	60.814	[nm]

(commonly nitrogen) onto the surface of a material. The acronym BET refers to the names of the scientists who introduced the process in the 1930s. The quantity of gas adsorbed under different pressures is employed to calculate the particular surface area of the material, which according to the BET formula is the total surface area per unit mass.

The BET analysis is commonly utilised in fields such as catalysis, materials science, and environmental science to determine the physical and chemical properties of porous materials, including catalysts, adsorbents, and nanomaterials. The technique provides crucial information on the pore size distribution, pore volume, and surface area of the material assessed, which could assist in understanding its performance and optimise its properties for specific applications.

The surface adsorption by the DPF waste in this study was evaluated though BET analyses. The results are summarised in Table 3. The surface area of the adsorbent was 0.75 $m^2 g^{-1}$. Moreover, the DPF adsorbent possessed an extremely high porosity surface profile, allowing a higher CR adsorption. The findings in the present study indicated that the DPF waste had the potential to be a decolorising agent in wastewater.

The X-ray diffraction analysis

An X-ray diffraction (XRD) evaluation was performed before and after the adsorption procedure, to determine the crystallisation of the DPF waste employed in the current study (see Figure 4). Evident changes in peak deviations, reduced peak strengths, and peak variations in certain regions were observed. Figure 4 illustrates three theta areas in which adsorption was the greatest (21.394, 30.769, and 53.806) with their corresponding d-values (0.4199, 0.29034, and 0.17023 nm) (Aziz et al., 2023). In this study, all XRD peaks recorded were employed to obtain the composite DPF waste with CR display. The DPF waste was found to possess a crystalline structure.

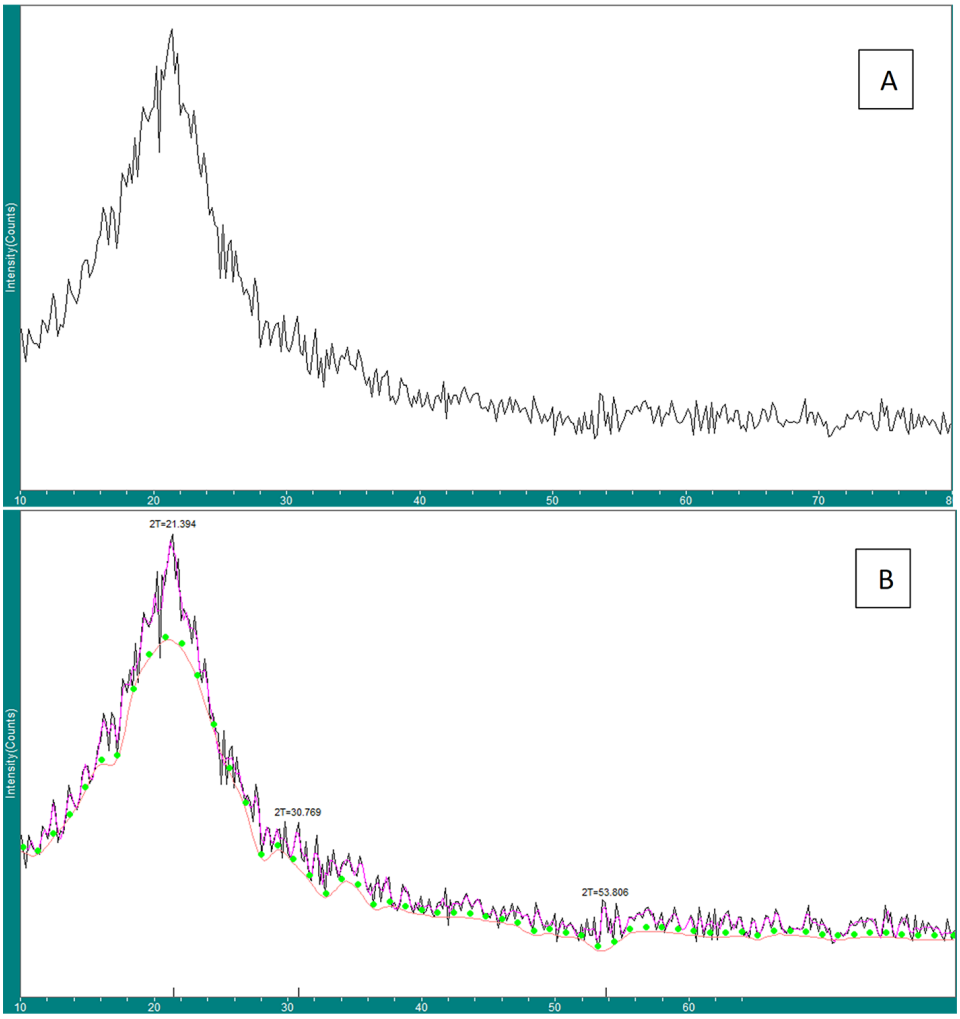

Figure 4. XRD analysis (a) raw DPF and (b) CR adsorption by DPF

Table 4. The Oxides component of DPF waste by XRF analysis

Oxides Component	DPF waste before adsorption (%)	DPF waste after adsorption (%)
SiO_2	3.090	3.616
Al_2O_3	0.681	0.795
Fe_2O_3	0.300	0.569
CaO	1.382	1.932
MgO	0.327	0.274
Na_2O	0.152	0.058
K_2O	0.151	0.178
TiO_2	0.072	0.104
MnO	0.014	0.021
P_2O_5	0.177	0.135

The X-ray fluorescence evaluation

An X-ray fluorescence (XRF) analysis is a non-destructive assessment for identifying the elemental makeup of a substance. The technique irradiates samples with X-rays, exciting their electrons and releasing fluorescent X-rays. The power and intensity of the X-rays emitted by the substances assessed allow determination of their elemental compositions. Different elements document distinct X-ray peaks at varied wavelengths of fluorescence intensities within each range. The lines relate to the focus of the element.

The XRF analysis could be conducted on various materials, such as metal, polymer, ceramic, minerals, and soil. Furthermore, the forensic science, research, and development fields and quality control, often employ the technique. The XRF is known also for its speed in producing accurate and reliable findings, ease of utilisation, and low cost compared to other analytical methods. Nevertheless, the method only allows surface analyses of materials and not the identification of trace minerals or lightweight components (such as hydrogen and helium).

The oxidised components of the DPF waste adsorbent prepared in this study before and after the CR adsorption process were examined with XRF spectroscopy (see Table 4). The results demonstrated that the DPF waste contained an increased relative silicon dioxide (SiO_2) amount. A high SiO_2 value indicates that a material contains significant plant fibre levels. On the other hand, a high aluminium oxide (Al_2O_3) content could suggest that a substance is comprised of alumina-rich plant fibres.

Alumina is commonly found in plant cell walls, contributing to the strength and structure of the fibres. The fibres from certain types of grasses or other plant species that grow in calcium- and magnesium-rich soils would record high calcium oxide (CaO) and magnesium oxide (MgO) contents. Conversely, low titanium dioxide (TiO_2), manganese oxide (MnO) and phosphorus pentoxide (P_2O_5) levels suggest that a waste material contains little to no plant fibres that are rich in

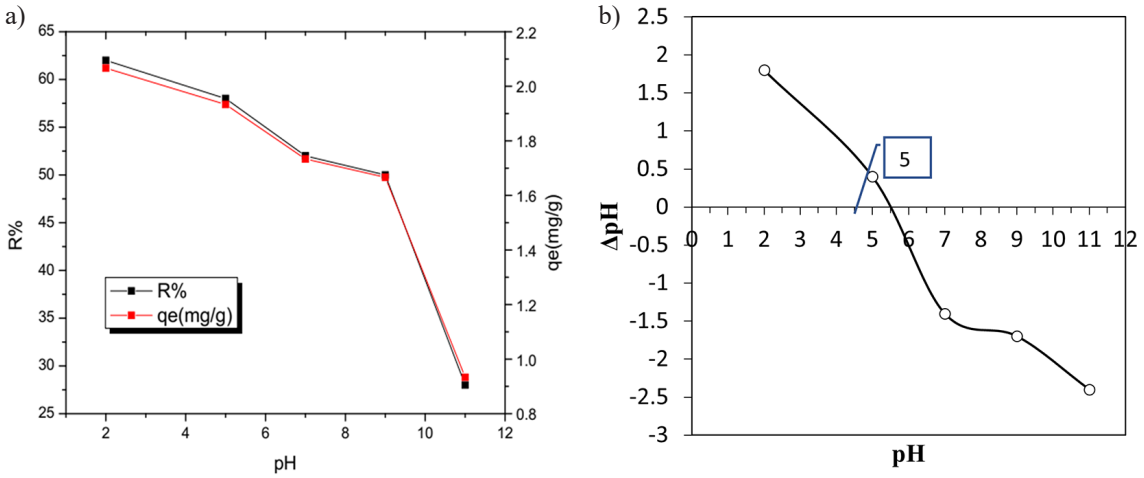

Figure 5. (a) Effect of pH value on CR removal efficiency and (b) Point of zero charge plot of DPF.

TiO_2. Nevertheless, not all plant fibres contain significant amounts of TiO_2, and its absence is not uncommon.

The effects of the different parameters

The effects of pH

In adsorption, the pH of an aqueous solution is the most critical component in determining the effectiveness of the process. In this study, the capacity of the DPF waste to adsorb CR dyes in aqueous solutions of 2–11 pH values was investigated. The CR dye adsorption at pH 2 was optimal, but the adsorption effectiveness progressively reduced with increasing alkalinity, with the lowest adsorption recorded at pH 11 (Alhares et al., 2023).

The influence of pH on the adsorption of CR fixed at 10 ppm, 3 g/L dosage, 3 mm particle size, and 3 h of shaking is depicted in Figure 5a. Zero charge pH value (pH_{pzc}) determination is critical to ascertain the optimal pH value of dye-polluted wastewater for adsorption (Chan et al., 2016). The figure was also crucial during electrostatic interaction mechanisms and pH compatibility of the solutions with the adsorption capacity assessments concerning the DPF waste in this study. A 5 pH_{pzc} was obtained in this study, with a lower positive charge and a higher negative charge (see Figure 5b). The higher pH_{pzc} value compared to pH indicated suitability for the adsorption of anionic dyes such as CR. Conversely, a lower pH_{pzc} figure is desirable for cationic dyes (Namasivayam et al., 1996).

The effects of interaction time

Figure 6a illustrates the effects of period of exposure of the CR to the DPF waste prepared in this study on the adsorption process. The adsorption was enhanced with a prolonged period, where the CR (fixed at 10 ppm, 3 g/L dosage, pH 2, and particle size was 0.075 mm) removal percentage reached 70% after 285 min of mixing. Nevertheless, the dye elimination rate in the

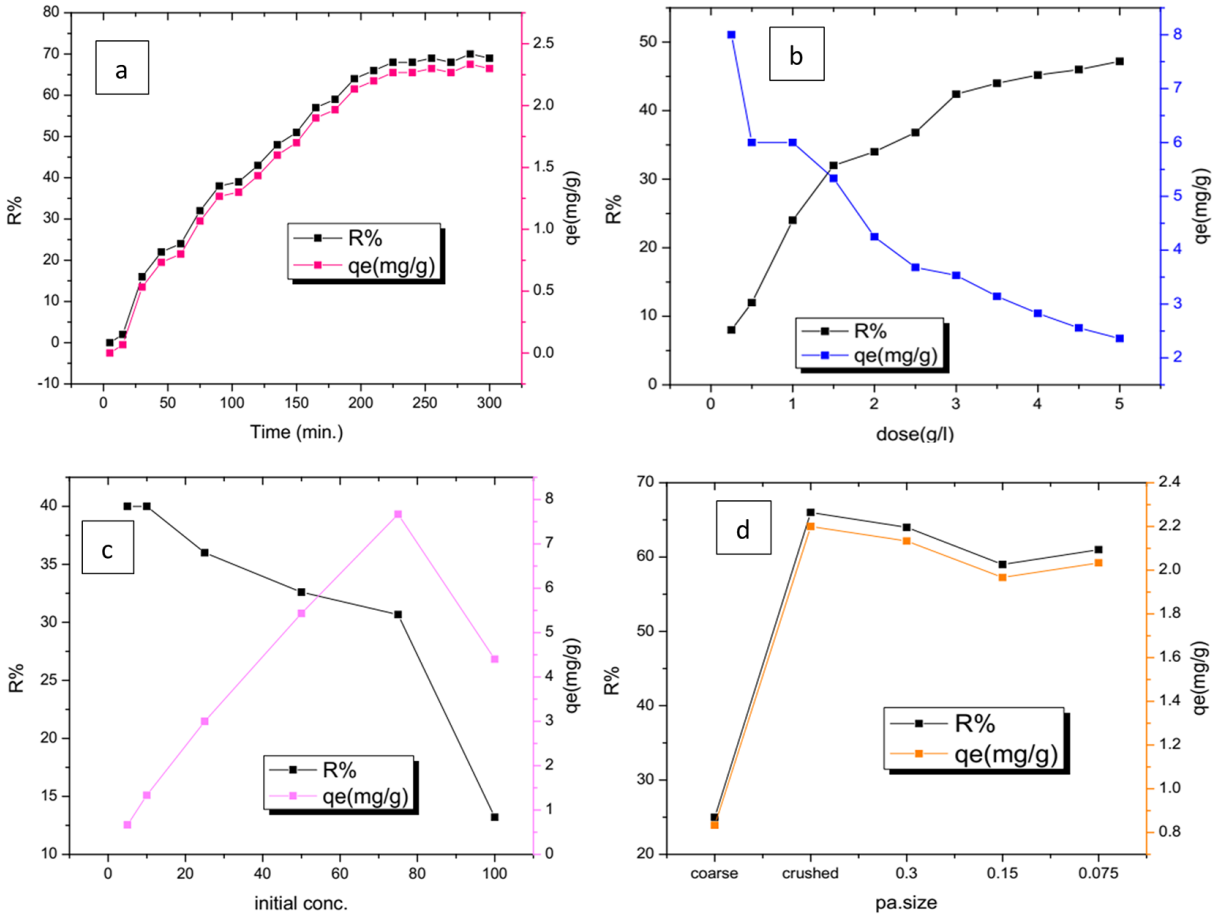

Figures 6. Batch process mode results: (a) effect of time period on CR removal, (b) effect of adsorbent dosage, (c) effect of the initial concentration of CR on the removal efficiency, (d) particle size effected on the CR dyes removal efficiency

initial few minutes was considerably higher due to the availability of pores in the first few minutes, which gradually decreased as time passed.

The influence of dosage

The present study maintained the initial concentration of the CR dye with a particle size of 0.3 mm at 25 ppm for 180 min to determine the efficacies of different adsorbent doses in removing the dye from water under controlled conditions. The impacts of altering the dosage on the dye removal effectiveness are depicted in Figure 6b. The dye elimination efficiency was significantly influenced with increasing adsorbent (DPF waste) levels.

The effects of the initial CR concentration

This study assessed the effects of the initial concentrations of the CR dye on the susceptibility of the DPF waste to adsorption. The effectiveness of colour removal from simulation wastewater by the adsorbent was evaluated by varying the concentration of the initial CR concentrations from 5 to 100 ppm. Resultantly, enhanced initial dye concentrations led to improved removal effectiveness (see Figure 6c). The observations might be due to the dye not competing with other substances to occupy the pores in the adsorbent. All experiments in this portion of the study were conducted at a fixed dosage of 3 g/L, 3 mm pore size, and a 3 h running duration.

The influence of the adsorbent particle size

The DPF adsorbent particle size prepared in the current study played an essential role in removing colours from wastewater when its dosage was maintained at 2 mg/L, the pH value was 2, and it was mixed for 3 h. Figure 6d demonstrates that the optimal particle size for the CR dye adsorption procedure was obtainable via the batch process. The maximum CR dye removed from wastewater was achieved when the 2 mm adsorbent was employed, reaching a 66% elimination.

The effects of temperature

The results of this study revealed that the quantity of heat affects adsorption. An increased temperature led to improved CR removal efficacy from wastewater. Figure 7 illustrates the dye elimination effectiveness at 25, 35, and 45 °C when the DPF waste was maintained at a constant dose of 3 mg/L, the dye starting concentration (C_0) was 10 ppm, the particle size was 0.075 mm, a mixing period of 5 h, and the pH was set at 2 throughout the experiment. A 72% dye removal was documented at 45 °C.

Adsorption kinetics

The present study experiment involved kinetic statistical analyses with pseudo-first-order and pseudo-second-order models to examine the CR adsorption mechanisms. The pseudo first-order model is represented by Equation 8 (Akar et al., 2009), while Table 5 demonstrates the pseudo-first-order kinetic.

$$\ln(q_e - q_t) = \ln q_e - k_1 t \quad (8)$$

The k_1 and q_e parameters were derived from the slopes and intercepts of the $\ln(q_e - q_t)$ against (vs) t (see Table 5), where q_e (mg/g) represents the equilibrium adsorption capacity, q_t (mg/g) denotes the adsorption capacity, and t (min) is the adsorption time, k_1 (l/min). The DPF waste recorded correlation coefficients (R^2) of 0.89, 0.87, and 0.91

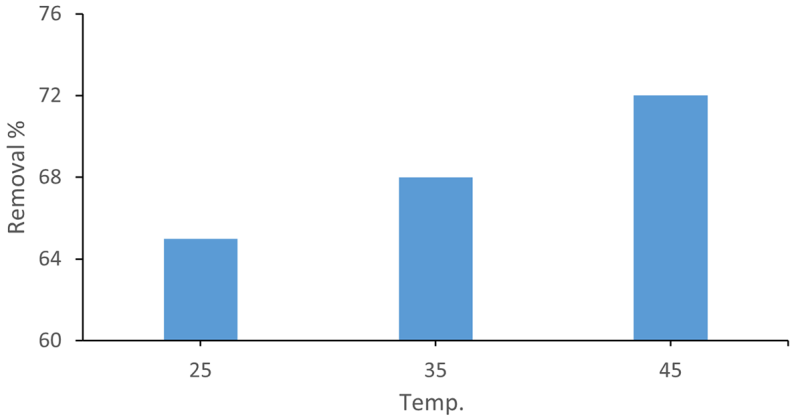

Figure 7. Effect of temperature on the removal efficiency of CR

when the q_{exp} were 2.4, 3.1, and 6.0, respectively. The low adjusted R^2 values and significant consistency between the estimated and actual $q_{e,\ exp}$ values indicated that the pseudo-first-order theory was not fitted for predicting the adsorption behaviours of CR onto the DPF adsorbent.

The pseudo-second-order model is represented by Equation 9 (Asgher and Bhatti, 2012; Salman et al., 2022), and table 5 illustrates its pseudo-second-order adsorption process. The intercepts and curves documented on the t/q_t vs t chart are listed in Table 5. On the basis of the results, the adjusted R^2 obtained were close to one. Furthermore, the $q_{e,cal}$ estimates were in excellent accordance with the $q_{e,exp}$ experimental results. The findings demonstrated that the pseudo-second-order kinetic model was applicable for the adsorption of CR onto the DPF waste.

$$\frac{t}{q_t} = \left(\frac{1}{k_2 q_e^2}\right) + \left(\frac{t}{q_e}\right) \tag{9}$$

where: q_e (mg/g) denotes equilibrium adsorption capacity;
q_t (mg/g) is the adsorption capacity;
t (min) represents adsorption time;
k_2 (mg/g·min) corresponds to constants.

Equation 10 is the formula suggested to represent intraparticle diffusion in this study (Belala et al., 2011; M-Ridha et al., 2022). On the other hand, table 5 depicts the kinetic graphs of the adsorption across various time intervals 5–300 min, C_0 = 10, 25, and 50 mg/L, pH = 7, DPF waste dose = 3 g/L dye solution, mixing speed = 150 rpm, and dye solution value temperature = 25 °C. The information collected in the present study is summarised in Table 5.

$$q_t = k_p t^{\frac{1}{2}} + C \tag{10}$$

where: C corresponds to the amount of an intercept (mg/g);
k_p is the intraparticle constant mass flow rate (mg/g·min$^{1/2}$).

Comparable adjusted R^2 of intraparticle diffusion from previous studies are listed in Table 5. According to the findings, the pseudo-first-order molecular diffusion concept was not related to the adsorbate in this study. At R^2 values of 0.98, 0.99, and 0.98 when C_o = 10, 25, 50 mg/L, the pseudo-second-order adsorption kinetics was able to attain optimum adsorption, revealing that they closely matched the values obtained throughout the period under consideration. Furthermore, the findings suggested a good agreement between the adsorbed observations and the pseudo-second-order kinetics models, validating the chemisorption-based adsorbed assumption of the model.

Adsorption isothermal

The adsorption kinetic demonstrates how adsorbate and adsorbed particles interact as well as provide the general capabilities of an adsorbent (Atiya et al., 2020; Ibrahim et al., 2022; Zhou et al., 2014). The experimental CR adsorption onto the DPF waste isotherm models at various degrees obtained in the present study is depicted in

Table 5. Pseudo-first-order, pseudo-second-order and intraparticle diffusion coefficient for CR adsorption by DPF

Model	Parameters					
Pseudo-first order	C_o (mg L^{-1})	q_{exp} (mg g^{-1})	q_{cal} (mg g^{-1})		K_1	R^2
	10	2.4	3.16		0.0118	0.8928
	25	3.1	4.25		0.0121	0.88
	50	6.0	7.15		0.0127	0.91
Pseudo-second order	C_o (mg L^{-1})	q_{exp} (mg g^{-1})	q_{cal} (mg g^{-1})		K_1	R^2
	10	2.4	3.62		0.0017	0.93
	25	3.1	2.55		0.0052	0.94
	50	6.0	7.22		0.0019	0.96
Intra-particle diffusion	C_o (mg L^{-1})	q_{exp} (mg g^{-1})	q_{cal} (mg g^{-1})	C	K_p	R^2
	10	2.4	2.47	0.157	-0.2514	0.983
	25	3.1	3.23	0.199	-0.2179	0.993
	50	6.0	6.19	0.332	0.4452	0.984

Figure 8, which employed CR contents ranging between 10 and 100 mg/L.

The findings from the adsorption equilibrium study were analysed with the Langmuir and Freundlich isotherm modelling techniques. The Langmuir model was founded on the premise that sorption occurs as a mono-layer on a face with various homogenous sites. Consequently, a model of Langmuir isotherm linear equation is expressed by Equation (11) (Mohammed et al., 2021; Mohammed and Mohammed-Ridha, 2021).

$$q_e = \frac{q_m\, b_l C_e}{1 + b_l C_e} \tag{11}$$

where: q_e (mg/g) denotes the equilibrium adsorption capacity;
q_m (mg/g) is the full monolayer adsorption capacity;
C_e (mg/L) represents the equilibrium CR concentration;
k_l corresponds to the heat of sorption with capability (L/mg).

$$R_L = \frac{1}{1 + K_L C_o} \tag{12}$$

The adsorption isotherms could be written as non-dimensional with specific R_L, which was employed judge the degree to which the adsorption was favourable [see Equation (12)] (Kandil and Ali, 2022; M-Ridha et al., 2021). The C_0 (mg/L), irreversibility (RL = 0), favourability (0 < RL < 1), unfavourability (RL > 1), and linearity (RL = 1) of the equilibrium data was determined based on the R_L value. Subsequently, the qm and KL values were be calculated by plotting a C_e/q_e vs Ce graph.

The Freundlich equilibrium (see Figure 8) adsorption formula posits that the surface of an adsorbent is heterogenous. Equation 13 mathematically expresses the Freundlich formula (Alhares et al., 2023). Table 6 lists the parameters for Langmuir and Freundlich isothermal equations employed in this study.

$$q_e = K_f C_e^{\frac{1}{n}} \tag{13}$$

where: q_e (mg/g) denotes the equilibrium adsorption capacity;
q_m (mg/g) represents the full monolayer adsorption capacity;
C_e (mg/l) is the equilibrium CR concentration;
k_l (l/mg), k_f (l/mg), and $1/n$ are constants.

Table 6. Freundlich and Langmuir coefficient for CR adsorption by DPF

Model	Parameters			
Langmuir	q_{exp} (mg g^{-1})	K_L (L mg^{-1})	R_L	R^2
	14.6	0.0118	0.09 – 0.1	0.992
Freundlich	K_F (mg g^{-1} (mg $L^{-1})^{-1/n}$)	n		R^2
	1.4	1.9		0.966

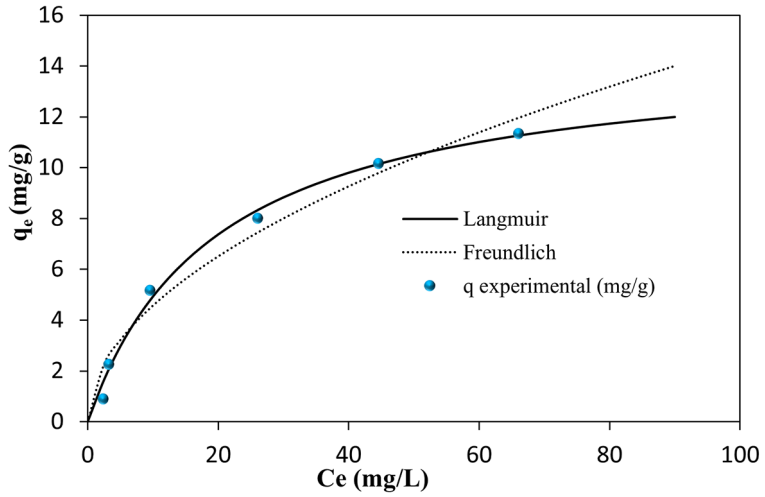

Figure 8. The Langmuir and Freundlich for the adsorption process

Table 7. Parameter of thermodynamic equation for CR adsorption

	ΔH° (kJ/mol)	ΔS° (kJ/mol. K)	ΔG° (kJ/mol)		
			25 °C	35 °C	45 °C
DPF	142.6128	1.6606	-352.483	-369.089	-385.694

The thermodynamic of adsorption

The CR adsorption onto the DPF adsorbent prepared in the current study was evaluated at different temperatures, where increased solution temperature led to improved dye adsorption. This study also included the thermodynamic dye adsorption from the solution assessments with several variables, including the Gibbs free energy change (ΔG^o) and enthalpy (ΔH^o) and entropic change (ΔS^o). Resultantly, the parameters described the thermodynamics through several equations, of which Equations (14) and (15) were the most critical (Depci et al., 2012; Namasivayam et al., 1996).

$$\Delta G^o = -RT\ln K_c \quad (14)$$

$$K_c = \frac{C_{ea}}{C_e} \quad (15)$$

$$\Delta G^o = \Delta H^o - T\Delta S^o \quad (16)$$

$$\ln K_c = \frac{\Delta S^o}{R} - \frac{\Delta H^o}{RT} \quad (17)$$

where: K_C – the equilibrium constant;
C_{ea} – represents the quantity of CR adsorption per volume of solution at stability in milligrams per litre;
R – a constant (8.314 J/mol.k).

The ΔH° and ΔS° parameters were derived from the intercept and slope of an ln K_C vs 1/T plot (see Figure 9), while Table 7 summarised the thermodynamic parameter values at different temperatures. The negative ΔG° values obtained at 25, 35, and 45 °C indicated that the process was feasible. Furthermore, this study achieved the chemisorption condition as the values obtained were within the −80 to −400 kJ/mol range. The significant ΔH° figures

Table 8. Parameter studied for continuous mode in COMSOL

No.	Parameter	Value
1	Fluid speed (mL/min)	25 75 125
2	Initial CR concentration (mol/m^3)	0.07171 0.035855 0.014342
3	Fixed-bed depth (m)	0.01 0.025 0.05 0.075 0.095

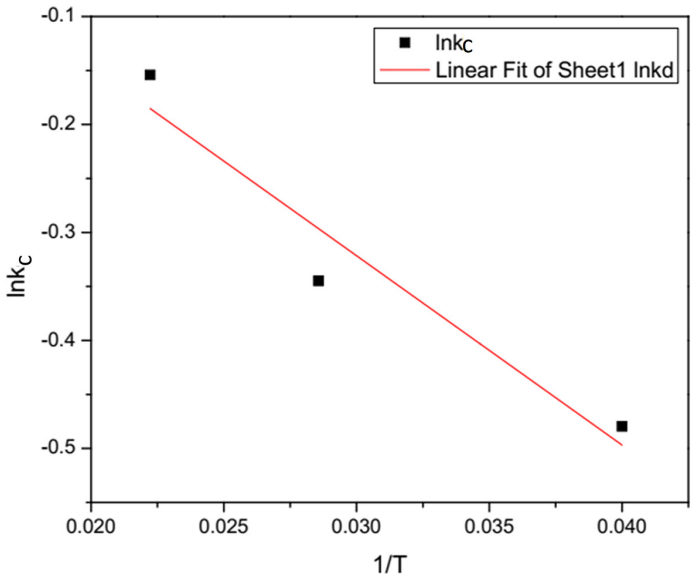

Figure 9. Thermodynamic equation of CR adsorption by DPF

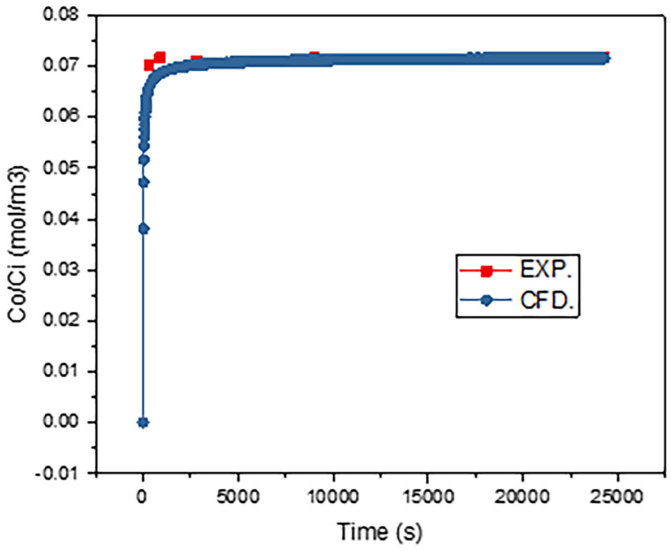

Figure 10. CFD simulation with experimental results

indicated the endothermic character of the adsorption system, while ΔS° positive numbers suggested rising randomness at phase boundaries during adsorption of the CR dye onto the DPF waste.

The continuous process simulation

An initial simulation process was conducted at 0.01, 0.025, 0.05, 0.075, and 0.095 m depth points at different flow speeds (25, 75, and 125 mL/min) and varied initial CR concentrations (0.07171,

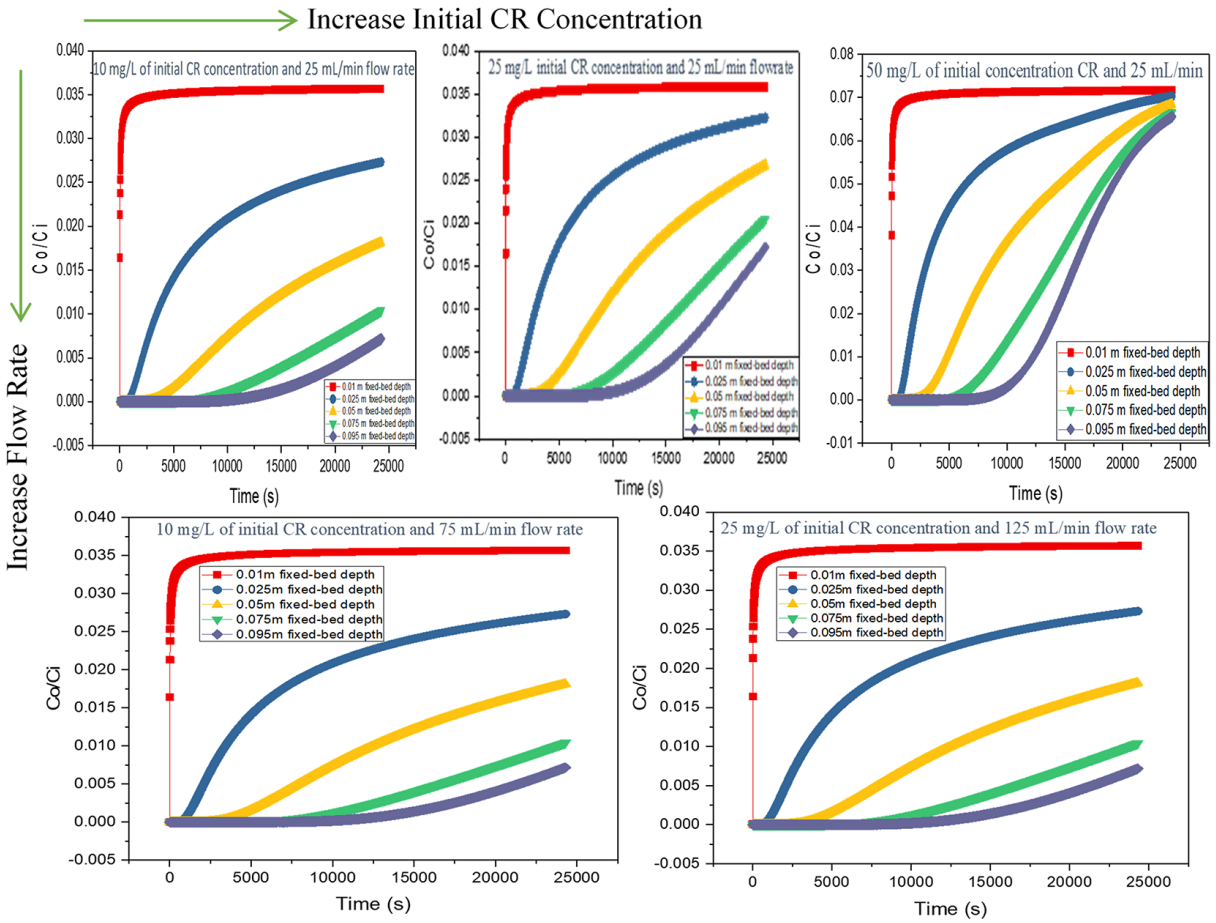

Figure 11. Parameters effects on CR adsorption

0.035855, and 0.014342 mol/m^3) for 24,300 sec. The results are summarised in Table 8.

The experiments in the current study were modelled in the COMSOL® program to simulate actual experiments. Figure 10 illustrates the simulation results of a 0.01 m tall, 25 mL/min flow rate, and 0.07171 mol/m^3 system. The computational fluid dynamics (CFD) simulation was then verified by comparing its anticipated outflow concentrations with the real experimental results of similar parameters. Both findings demonstrated excellent accordance, suggesting that the CFD simulation was accurate for generating insights into CR dye separation from wastewater.

Several factors, including initial CR dye concentrations in the wastewater and exposure period of the dye to the adsorbent influenced the CR dye adsorption process. Other conditions, such as column depth and fluid flow rate, also require consideration when studying continuous adsorption operations in fixed columns. Figure 11 illustrates the feasibility of dye adsorption in a continuous process based on the interactions of several parameters.

The results revealed that increased initial dye concentration led to improved effectiveness of the dye removal from wastewater, which might be due to the lack of competition between dye and other compounds to be adsorbed. Nonetheless, decreased removal percentage was documented when the liquid flow rate was increased as a low flow rate allows greater exposure time between the solution and the adsorbent.

The depth of the liquid significantly impacted the dye removal process, where the process was enhanced when the height of the adsorbent material in the fixed bed column was increased. Furthermore, the results suggested that the CR dye solution was exposed to the dyes with the filling. The greater the exposure of the dyes with the filling of the adsorbent material, the more liquid was adsorbed; thus the process improved with an enhanced adsorption column length. Exposure time between the dye-polluted solution and the adsorbent also affected the absorption effectiveness, where a longer period increased the effectiveness of dye removal.

CONCLUSIONS

The current study successfully introduced a novel approach to recycling palm waste as an adsorbent for various dyes, including CR. This study demonstrated that it was possible to recover the fibres from agricultural date palm leftovers during the harvest season, particularly in the south of Baghdad, Iraq. The fibres could then be employed as an additive for the commonly utilised CR dye.

The findings in the present study revealed a favourable dye uptake potential by the DPF. Nevertheless, the optimal conditions depended on the pH, contact duration, temperature, initial concentration of dyes in wastewater, particle size, and mixing time. The adsorption results obtained in this study were also subjected to a thorough examination utilising the Langmuir and Freundlich isotherms as models. Resultantly, DPF waste was the most effective method of eliminating CR dyes during wastewater treatments. Furthermore, the DPF waste, employed as an adsorbent, is an ecologically benign substance that is easily obtainable and does not require any industrial overhead.

The current study constructed a fixed-bed reactor to remove CR dye from sewage water continuously. The COMSOL® software was employed to simulate the system. The CFD simulation findings were compared to the actual results. The data obtained exhibited an excellent match, achieving nearly 99%. Several system factors, including the time required to remove dyes from wastewater, the influence of starting CR concentrations, flow rate, and the effects of filler height, were also investigated and discussed in this study.

Acknowledgment

Authors would like to express their gratitude for the technical support provided by the Northern Technical University during this work, especially the Department of Environment and Pollution Techniques Engineering. The authors would like to thank the College of Engineering, University of Baghdad. The authors also would like to thank the Universiti Kebangsaan Malaysia for financial support through the Dana Impak Perdana with grant number DIP-2021-008.

REFERENCES

1. Abed, K.M., Hayyan, A., Elgharbawy, A.A.M., Hizaddin, H.F., Hashim, M.A., Hasan, H.A., Hamid, M.D., Zuki, F.M., Saleh, J., Aldaihani, A.G.H., 2022. Palm Raceme as a Promising Biomass Precursor for Activated Carbon to Promote Lipase Activity with the Aid of Eutectic Solvents. Molecules 27, 8734.

2. Ahmad, M.A., Alrozi, R., 2011. Removal of malachite green dye from aqueous solution using rambutan peel-based activated carbon: Equilibrium, kinetic and thermodynamic studies. Chem. Eng. J. 171, 510–516. https://doi.org/10.1016/J.CEJ.2011.04.018
3. Akar, S.T., Gorgulu, A., Kaynak, Z., Anilan, B., Akar, T., 2009. Biosorption of Reactive Blue 49 dye under batch and continuous mode using a mixed biosorbent of macro-fungus Agaricus bisporus and Thuja orientalis cones. Chem. Eng. J. 148, 26–34. https://doi.org/10.1016/j.cej.2008.07.027
4. Al-bayati, M.H., Najim, S.T., 2022. Water Purification By Removing Chemical Materials From Water By Electrochemical Methods 1, 2–5.
5. Alhares, H.S., Shaban, M.A.A., Salman, M.S., M-Ridha, M.J., Mohammed, S.J., Abed, K.M., Ibrahim, M.A., Al-Banaa, A.K., Hasan, H.A., 2023. Sunflower Husks Coated with Copper Oxide Nanoparticles for Reactive Blue 49 and Reactive Red 195 Removals: Adsorption Mechanisms, Thermodynamic, Kinetic, and Isotherm Studies. Water, Air, Soil Pollut. 234, 35. https://doi.org/10.1007/s11270-022-06033-6
6. Asgher, M., Bhatti, H.N., 2012. Removal of reactive blue 19 and reactive blue 49 textile dyes by citrus waste biomass from aqueous solution: Equilibrium and kinetic study. Can. J. Chem. Eng. 90, 412–419. https://doi.org/10.1002/cjce.20531
7. Atiya, M.A., M-Ridha, M.J., Saheb, M.A., 2020. Removal of Aniline Blue from Textile Wastewater using Electrocoagulation with the Application of the Response Surface Approach. Iraqi J. Sci. 61, 2797–2811. https://doi.org/10.24996/ijs.2020.61.11.4
8. Aziz, G.M., Hussein, S.I., M-Ridha, M.J., Mohammed, S.J., Abed, K.M., Muhamad, M.H., Hasan, H.A., 2023. Activity of laccase enzyme extracted from Malva parviflora and its potential for degradation of reactive dyes in aqueous solution. Biocatal. Agric. Biotechnol. 50, 102671. https://doi.org/10.1016/j.bcab.2023.102671
9. Belala, Z., Jeguirim, M., Belhachemi, M., Addoun, F., Trouvé, G., 2011. Biosorption of basic dye from aqueous solutions by Date Stones and Palm-Trees Waste: Kinetic, equilibrium and thermodynamic studies. Desalination 1–3, 80–87. https://doi.org/10.1016/J.DESAL.2010.12.009
10. Chan, S.L., Tan, Y.P., Abdullah, A.H., Ong, S.T., 2016. Equilibrium, kinetic and thermodynamic studies of a new potential biosorbent for the removal of Basic Blue 3 and Congo Red dyes: Pineapple (Ananas comosus) plant stem. J. Taiwan Inst. Chem. Eng. C, 306–315. https://doi.org/10.1016/J.JTICE.2016.01.010
11. Chebli, D., Bouguettoucha, A., Mekhalef, T., Nacef, S., Amrane, A., 2014. Valorization of an agricultural waste, Stipa tenassicima fibers, by biosorption of an anionic azo dye, Congo red. New pub Balaban 54, 245–254. https://doi.org/10.1080/19443994.2014.880154
12. Chen, Zhengxian, Wang, T., Jin, X., Chen, Zuliang, Megharaj, M., Naidu, R., 2013. Multifunctional kaolinite-supported nanoscale zero-valent iron used for the adsorption and degradation of crystal violet in aqueous solution. J. Colloid Interface Sci. 398, 59–66. https://doi.org/10.1016/J.JCIS.2013.02.020
13. Ciardelli, G., Corsi, L., Marcucci, M., 2001. Membrane separation for wastewater reuse in the textile industry. Resour. Conserv. Recycl. 31, 189–197. https://doi.org/10.1016/S0921-3449(00)00079-3
14. Depci, T., Kul, A.R., Önal, Y., 2012. Competitive adsorption of lead and zinc from aqueous solution on activated carbon prepared from Van apple pulp: Study in single- and multi-solute systems. Chem. Eng. J. 200–202, 224–236. https://doi.org/10.1016/J.CEJ.2012.06.077
15. Gardiner, D.K., Borne, B.J., 1978. Textile Waste Waters: Treatment and Environmental Effects. J. Soc. Dye. Colour. 94, 339–348. https://doi.org/10.1111/J.1478-4408.1978.TB03420.X
16. Hasan, I., Ahamd, R., 2019. A facile synthesis of poly (methyl methacrylate) grafted alginate@Cys-bentonite copolymer hybrid nanocomposite for sequestration of heavy metals. Groundw. Sustain. Dev. 8, 82–92. https://doi.org/10.1016/J.GSD.2018.09.003
17. Ibrahim, M.A., Shaban, M.A.A., Hasan, Y.R., M-Ridha, M.J., Hussein, H.A., Abed, K.M., Mohammed, S.J., Muhamad, M.H., Hasan, H.A., 2022. Simultaneous Adsorption of Ternary Antibiotics (Levofloxacin, Meropenem, and Tetracycline) by SunFlower Husk Coated with Copper Oxide Nanoparticles. J. Ecol. Eng. 23, 30–42.
18. Kandil, H., Ali, H., 2022. Simultaneous Removal of Cationic Crystal Violet and Anionic Reactive Yellow Dyes using eco-friendly Chitosan Functionalized by Talc and Cloisite 30B. J. Polym. Environ. 1–22. https://doi.org/10.1007/S10924-022-02682-0/TABLES/5
19. Ledakowicz, S., Solecka, M., Zylla, R., 2001. Biodegradation, decolourisation and detoxification of textile wastewater enhanced by advanced oxidation processes. J. Biotechnol. 89, 175–184. https://doi.org/10.1016/S0168-1656(01)00296-6
20. M-Ridha, M.J., Faeq Ali, M., Hussein Taly, A., Abed, K.M., Mohammed, S.J., Muhamad, M.H., Abu Hasan, H., 2022. Subsurface Flow Phytoremediation Using Barley Plants for Water Recovery from Kerosene-Contaminated Water: Effect of Kerosene Concentration and Removal Kinetics. Water 14, 687. https://doi.org/10.3390/w14050687
21. M-Ridha, M.J., Zeki, S.L., Mohammed, S.J., Abed,

K.M., Hasan, H.A., 2021. Heavy Metals Removal from Simulated Wastewater using Horizontal Subsurface Constructed Wetland. J. Ecol. Eng. 22, 243–250.

22. Malik, P.K., Saha, S.K., 2003. Oxidation of direct dyes with hydrogen peroxide using ferrous ion as catalyst. Sep. Purif. Technol. 31, 241–250. https://doi.org/10.1016/S1383-5866(02)00200-9
23. Mohammed, S.J., M-Ridha, M.J., Abed, K.M., Elgharbawy, A.A.M., 2021. Removal of levofloxacin and ciprofloxacin from aqueous solutions and an economic evaluation using the electrocoagulation process. Int. J. Environ. Anal. Chem. 1–19.
24. Mohammed, S.J., Mohammed-Ridha, M.J., 2021. Optimization of levofloxacin removal from aqueous solution using electrocoagulation process by response surface methodology. Iraqi J. Agric. Sci. 52, 204–217. https://doi.org/10.36103/IJAS.V52I1.1252
25. Namasivayam, C., Muniasamy, N., Gayatri, K., Rani, M., Ranganathan, K., 1996. Removal of dyes from aqueous solutions by cellulosic waste orange peel. Bioresour. Technol. 57, 37–43. https://doi.org/10.1016/0960-8524(96)00044-2
26. Nouh, S.A., Lau, K.K., Shariff, A.M., 2010. Modeling and simulation of fixed bed adsorption column using integrated CFD approach. J. Appl. Sci. 10, 3229–3235. https://doi.org/10.3923/jas.2010.3229.3235
27. Salman, M.S., Alhares, H.S., Ali, Q.A., M-Ridha, M.J., Mohammed, S.J., Abed, K.M., 2022. Cladophora Algae Modified with CuO Nanoparticles for Tetracycline Removal from Aqueous Solutions. Water, Air, Soil Pollut. 233, 321. https://doi.org/10.1007/s11270-022-05813-4
28. Saravanan, A., Kumar, P.S., Jayasree, R., Jeevanantham, S., 2020. Membrane separation technologies for downstream processing, Biovalorisation of Wastes to Renewable Chemicals and Biofuels. Elsevier Inc. https://doi.org/10.1016/b978-0-12-817951-2.00021-3
29. Solangi, Z.A., Bhatti, I., Qureshi, K., 2022. A Combined CFD-Response Surface Methodology Approach for Simulation and Optimization of Arsenic Removal in a Fixed Bed Adsorption Column. Processes 10. https://doi.org/10.3390/pr10091730
30. Subramaniam, R., Kumar Ponnusamy, S., 2015. Novel adsorbent from agricultural waste (cashew NUT shell) for methylene blue dye removal: Optimization by response surface methodology. Water Resour. Ind. 11, 64–70. https://doi.org/10.1016/J.WRI.2015.07.002
31. Tan, K.B., Vakili, M., Horri, B.A., Poh, P.E., Abdullah, A.Z., Salamatinia, B., 2015. Adsorption of dyes by nanomaterials: Recent developments and adsorption mechanisms. Sep. Purif. Technol. 150, 229–242. https://doi.org/10.1016/J.SEPPUR.2015.07.009
32. Uddin, M.T., Rahman, M.A., Rukanuzzaman, M., Islam, M.A., 2017. A potential low cost adsorbent for the removal of cationic dyes from aqueous solutions. ApWS 7, 2831–2842. https://doi.org/10.1007/S13201-017-0542-4
33. Yagub, M.T., Sen, T.K., Ang, H.M., 2012. Equilibrium, kinetics, and thermodynamics of methylene blue adsorption by pine tree leaves. Water. Air. Soil Pollut. 223, 5267–5282. https://doi.org/10.1007/S11270-012-1277-3/METRICS
34. Zhang, W., Yan, H., Li, H., Jiang, Z., Dong, L., Kan, X., Yang, H., Li, A., Cheng, R., 2011. Removal of dyes from aqueous solutions by straw based adsorbents: Batch and column studies. Chem. Eng. J. 168, 1120–1127. https://doi.org/10.1016/J.CEJ.2011.01.094
35. Zhang, Z., O'Hara, I.M., Kent, G.A., Doherty, W.O.S., 2013. Comparative study on adsorption of two cationic dyes by milled sugarcane bagasse. Ind. Crops Prod. 42, 41–49. https://doi.org/10.1016/J.INDCROP.2012.05.008
36. Zhou, F., Cheng, Y., Gan, L., Chen, Z., Megharaj, M., Naidu, R., 2014. Burkholderia vietnamiensis C09V as the functional biomaterial used to remove crystal violet and Cu(II). Ecotoxicol. Environ. Saf. 105, 1–6. https://doi.org/10.1016/J.ECOENV.2014.03.028